Analysis of spray induced flow of gasoline direct injection (GDI) nozzle by means of time-resolved Fluorescence-Particle Image Velocimetry

N. Kling[1,2*], L. Opfer[1], J. Kriegseis[2], P. Rogler[1]
[1]Robert Bosch GmbH, Powertrain Solutions, Schwieberdingen, Germany
[2]Institute of fluid mechanics (ISTM), Karlsruhe Institute of Technology (KIT), Germany

Abstract

The development of modern gasoline direct injection (GDI) nozzles demands profound knowledge about the mechanisms of spray transport in order to minimize emissions and maximize fuel efficiency. To receive a fundamental understanding about spray transport, the present study investigates spray induced flow of a two-hole research nozzle. Air entrainment, spray-air interaction and jet-to-jet interaction are analyzed by means of time-resolved Fluorescence-Particle Image Velocimetry (FPIV).

In order to achieve phase discrimination, optical filtering is applied by doping the gaseous phase with fluorescent seeding particles. The investigation considers near field and global spray characteristics by using different field of views and optical magnifications.

Flow features such as displacement and entrainment are identified and localized, providing a description of strength, growth and propagation. The exchange of momentum between spray and gas indicates jet-to-jet interaction by attraction of separate spray plumes. The investigation demonstrates a dependency between spray hole inclination angle and entrainment flow. Spray plumes with smaller inclination angels tend to be more attracted than spray plumes with higher inclination angels. A disparity of momentum exchange is observed

Keywords: Spray induced flow, entrainment, spray-air interaction, jet-to-jet interaction, Particle Image Velocimetry, GDI

Introduction

In modern combustion engine development the mechanisms of spray transport play a significant role in the optimization of fuel consumption and emissions [1, 2]. Mixture preparation and combustion are directly affected by the underlying characteristics of spray transport. Central aspects of spray layout and spray targeting are the prevention of wall wetting and the realization of spacious mixture homogenization. Spray transport is described by multiple aspects. Conditioned on the mechanism of internal nozzle flow, cavitation and atomization spray propagation is controlled by the interaction between spray and ambient gas [3]. In the context of spray transport the interaction is primarily described by the exchange of momentum. The momentum exchange between spray and gas forms a spray induced flow and has retroactive effects on the propagation of spray. The influence of ambient gas flow increases with smaller droplet sizes, therefore the spray induced flow affects the spray propagation in particular at far-field developed spray regions.

As a consequence of spray air interaction, separate spray plumes of multi-hole sprays are linked and communicate with each other. Depending on the conditions, injector design, spray layout and spray targeting, phenomena of jet-to-jet attraction and spray contraction are observed. Under the presence of strong jet-to-jet interaction spray propagation deviates from its original spray targeting.

Previous investigations of spray induced flow have been conducted by utilizing Particle Image Velocimetry. Kozma et al. [4] characterized air entrainment of a high pressure diesel spray. Rottenkolber et al. [5] investigated spray contraction of a hollow-cone spray whilst spray-air interaction of multiple injections have been examined by Sauter et al. [6].

In order to receive a profound understanding of spray transport and its underlying mechanism such as spray air interaction and jet-to-jet interaction in the present work an investigation of spray induced flow and its effects on spray transport are analysed by means of time-resolved Stereo-Particle Image Velocimetry.

In order to account for the enhanced requirements of two-phase flow fluorescent seeding particles and optical filtering is applied. The investigation is performed with a GDI two-hole research sample. In comparison to multi-hole sprays it provides extended optical access and a reduction of complexity. The simplification allows the isolation and extraction of singular jet-to-jet interaction.

The investigation comprises global, as well as near field measurements at normal temperature and pressure (NTP) conditions. Spatio-temporal air entrainment and displacement are examined on the basis of polar coordinates. The composition of spray induced flow is characterized by the quality of flow features. The influence of shot-to-shot

deviation in regard of air entrainment and displacement is identified and localized. A characterization of spray air interaction and jet-to-jet interaction is conducted by momentum exchange analysis.

Measurement setup

The investigation of spray induced flow is performed in an optical accessible pressure chamber. The pressure chamber provides an inert nitrogen atmosphere. In figure 1 the measurement setup is illustrated. The injector placement is at top centre position. The orientation of the injector and the measurement plane of the PIV setup are aligned with the spray plumes of the two-hole nozzle.

The Particle Image Velocimetry setup consists of a high-speed camera and a dual-cavity Nd:YAG laser. The laser operates with a wavelength of 532 nm. For different optical magnification the camera is equipped with a AF-S NIKKOR 105 mm lens for global spray imaging and with a combination of a NIKKOR 200 mm lens and a 2x teleconverter for near field imaging. In order to achieve phase discrimination and contrast enhancement fluorescent tracer particles and optical filters are utilized. The tracer particles are a solution of fluorescent laser dye (DCM) and Propylene Carbonate as a solvent [5]. The fluorescent emission is characterised by a strong frequency shift allowing distinct separation and high yield of laser intensity. The optical filtering is realised with an OD 4 short-pass filter with a cut-off wavelength of 600 nm. As a consequence of two-phase flow multiple scattering deforms and expands the original laser light sheet leading to an illumination of out of focus particles. The contribution of out of focus particles in regard of PIV cross correlation analysis is limited to the dimension of depth of correlation. The magnitude is referred as two times depth of field [7, 8].

The thermodynamic operation conditions of the measurements are 1 bar backpressure, 25 °C chamber temperature, 200 bar injection pressure and 25 °C fuel temperature. The experiments are conducted with n-Heptane as fuel. The two-hole nozzle describes a research sample with spray hole inclination angles of 10 and 50 degrees. A summary of the measurement conditions is shown in table 1.

The assessment of velocity vectors is conducted by a multi-grid multi-pass cross-correlation algorithm using an interrogation area overlap of 50% [9]. The final size of the interrogation areas is 24x24 pixels. For the promotion of data validity a normalized median filter (3x3 neighbourhood) [10] is applied to detect and remove spurious vectors.

Table 1 Measurement conditions

Gaseous phase	
Species	N_2
Backpressure (absolute)	1 bar
Temperature	25 °C
Liquid Fuel	
Species	n-Heptane
Pressure (absolute)	200 bar
Temperature	25 °C

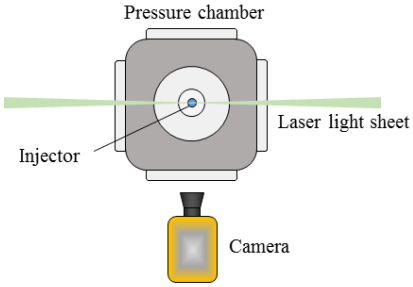

Figure 1 Schematic illustration of the experimental assembly; Planar Particle Image Velocimetry setup

Results and Discussion

The temporal evolution of spray induced flow in case of an individual injection event is shown in figure 2. The velocity fields indicate characteristic flow patterns revealing displacement in the vicinity of spray plume tip and entrainment at lateral positions. As a result of spray air interaction, the velocity fields show small scale structures at the proximity of spray. The spray transport of the individual injection events deviate due to shot-shot deviations.

In order to provide a qualitative and quantitative description of air entrainment and displacement the flow field is transformed from Cartesian coordinates to polar coordinates. The origin of the polar coordinate system is defined as the injector tip position (see figure 2). The transformation to polar coordinates allows the decomposition of the velocity vectors in radial and angular components. Assuming conical spray plume geometry the angular velocity component represents the normal net flow in lateral spray domain. The polar coordinates specify the spatial dimensions as a function of injector tip distance and corresponding angle. This provides the allocation to spray relevant quantities such as penetration and spray angle.

In figure 3 the angular velocity distributions of three consecutive instants of time are shown. The present image section comprises an area of a single spray plume. The angular velocity distributions identify and localize domains of displacement and entrainment. The separation of displacement and entrainment are indicated by a change of

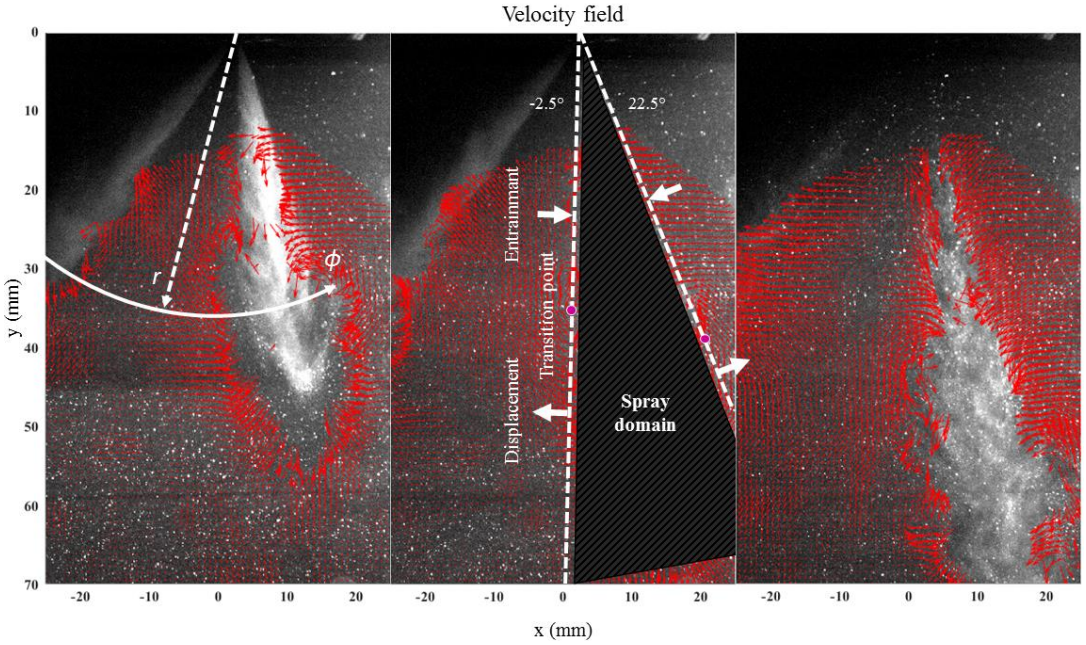

Figure 2 Spray induced flow of a single injection event; background: raw image of laser light sheet with particle images; Time after start of injection: left t = 1.4µs, middle t = 2.0µs, right t = 2.4µs; left: polar coordinate system; middle: dashed lines φ = -2.5° and φ = 22.5°; arrows represent displacement and entrainment; hatched area marks spray domain; purple points: transition points

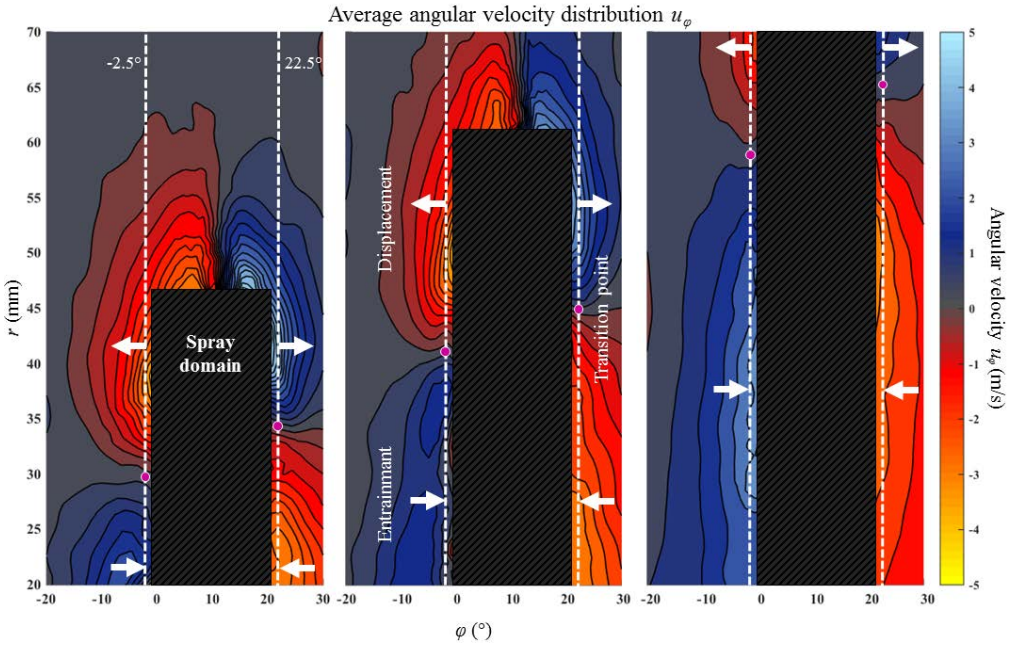

Figure 3 Average angular velocity u_φ depending based on polar coordinates; Time after start of injection: left t = 1.4µs, middle t = 2.0µs, right t = 2.4µs; dashed lines φ = -2.5° and φ = 22.5°; arrows represent displacement and entrainment; hatched area marks spray domain; purple points: transition points

sign. The angular velocity distributions depict axially symmetric similarities. However, the location of separation and the strength of angular velocity are different.

In figure 4 and 5 the temporal evolutions of angular velocities and its corresponding standard deviations are shown for constant angles of φ = -2.5° and φ = 22.5°. The angles are selected in order to have the same absolute distance to the corresponding spray hole inclination angle which is φ = 10°. The angles represent the external and internal sides of the spray plume in reference to the two-hole spray. The angular velocity distribution shows the spatial development of displacement and entrainment flow. Based on the curvature of the contour lines the

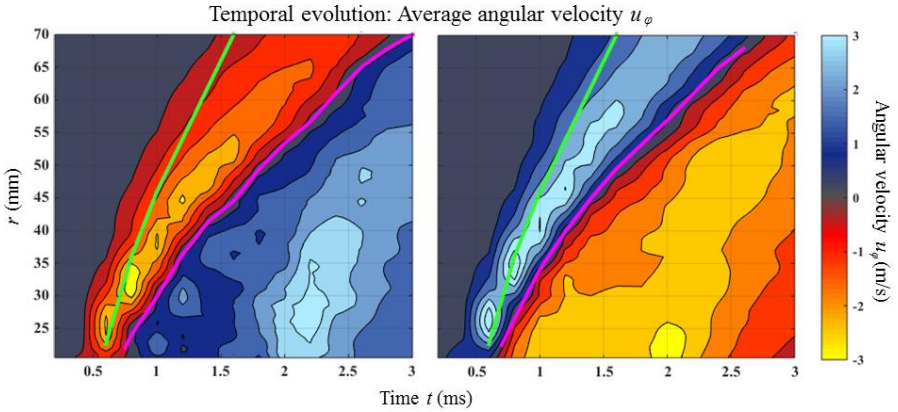

Figure 4 Temporal evolution of angular velocity u_φ; left: φ = -2.5°, right: φ =22.5°; green line - instantaneous spray tip position; purple line – vanishing radial velocity representing turning point between displacement and entrainment

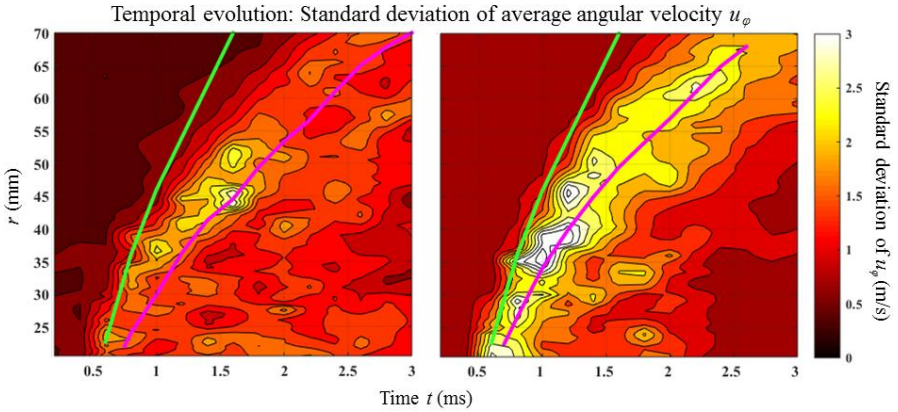

Figure 5 Temporal evolution of the standard deviation of angular velocity u_φ; left: φ = -2.5°, right: φ = 22.5°; green line - instantaneous spray tip position; purple line - vanishing radial velocity representing turning point between displacement and entrainment

motion of flow features decelerates. The quality of deceleration is dependent on position. The green curve illustrates the position of the instant spray tip whereas the magenta curve outlines the position of the transition point. By comparison the movement of the transition point is decelerated to a greater extent. The spatial difference in deceleration leads to an elongation of flow features. The radial size of the displacement area expands. Simultaneously the magnitude of the angular velocities decline. The displacement area and the entrainment area constitute a vortex ring. The observation of expansion and attenuation is the consequence of impulse diffusion and respectively vorticity diffusion. In figure 5 the ratios between the radial positions of the spray tip and the transition points is pictured as a function of time. The ratios are roughly constant and describe an approximate medium proportion of about 3:7. The standard deviations of the angular velocities depict the strongest values in the vicinity of the transition points. Besides shot-to-shot variance this is due to high spatial gradients in the surrounding domain. The shot-to-shot deviations are more prominent in the areas of displacement and transition to entrainment than in upstream regions. Among various factors of influence such as inner nozzle flow atomization, turbulence and spray air interaction early stage deviations propagate and accumulate leading to stronger differences in far-field developed-spray regions.

Comparing the angular velocity distributions of φ = -2.5° and φ = 22.5° the velocity magnitudes of the external flow field is higher than the internal flow field. As the flow is assumed as incompressible due to low mach numbers the impulse transport from external is stronger than from internal. This implies a greater momentum exchange by external flow and a deflection of the spray plume towards the second spray plume indicating jet-to-jet interaction. In figure 6 the near field of the corresponding spray induced flow is shown. The velocity field is averaged over several injection events eliminating the influence of shot-to-shot variances. The magnitude as well as the direction of the velocity vectors reveal a stronger momentum exchange between spray and gas from external flow as compared to the central flow region. This is in conjunction to the global velocity field observations. Furthermore, in the near field the momentum exchange is dependent on the inclination angles of the spray holes. For smaller inclination angle a greater disparity between external and internal velocity magnitudes is observed, whereas at

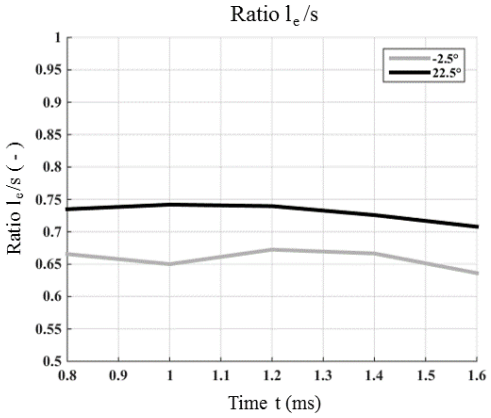

Figure 6 Ratio of transition point distance and radial penetration; gray line φ = -2.5°, black line φ = 22.5°

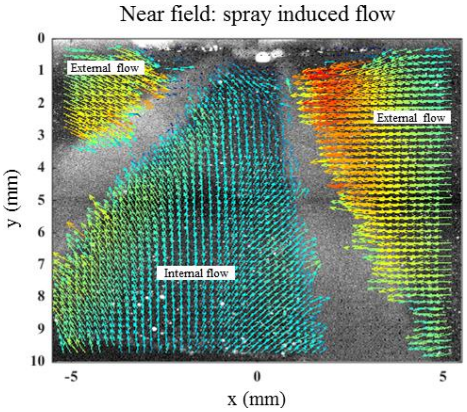

Figure 7 Near field image of spray induced flow; background: raw image of laser light sheet; external and internal flow regions

higher inclination angle a comparatively light difference is identified. The spray induced flow in the near field implies a mutual attraction of spray plumes. The spray plume with smaller inclination angle notices a stronger deflective momentum exchange.

Summary and Conclusions

Time-resolved Particle Image Velocimetry measurements have been performed in order to investigate the spray induced flow, the spray air interaction and the jet-to-jet interaction of a GDI two-hole research sample. The investigation comprises multiple measurements including global and near field measurements. In order to achieve phase discrimination and contrast enhancement fluorescent tracer particles and optical filters are applied.

By assuming conical spray plume geometry and utilizing polar coordinates a comprehensive description of air net flow representing displacement and air entrainment is attained. Based on the representation of net flow displacement and entrainment areas, corresponding transition points are identified and localized. The temporal evolution of flow features indicate different propagation speeds. The ratio between transition point distance and instant penetration is approximately 3:7. It is nearly constant over time. Shot-to-shot deviations concentrate at frontal areas of displacement and entrainment and particularly in the vicinity of transition.

Considering the velocity magnitudes of the net flow higher velocities are observed at the external side as compared to the internal side. Assuming incompressible flow due to low mach numbers the difference of the velocity magnitudes exhibit higher exchange of momentum from external flow. The difference of momentum exchange induces a deflection of spray transport. The momentum exchange implies jet-to-jet interaction due to mutual attraction.

References

[1] Baecker H., Lerch J. and Kroiss M., *Untersuchungen zur Benzindirekteinspritzung vor dem Hintergrund zukünftiger Emissions- und Verbrauchsanforderungen*, Haus der Technik, (2011)

[2] Zhao F., Lai M. C. and Harrington D. L., *Automotive spark-ignition direct-injection gasoline engines*, Progress in Energy and Combustion Science 25, pp. 437–562, (1999)

[3] Ashgriz N., *Handbook of Atomization and Sprays,* Springer Boston Ma, (2011)

[4] Kozma, J. and Farrell, P., *Air Entrainment in a High Pressure Diesel Spray*, SAE Technical Paper 971620, (1997)

[5] Rottenkolber G., Gindele J., Raposo J., Dullenkopf K., Hentschel W., Wittig S., Spicher U. and Merzkirch W., *Spray analysis of a gasoline direct injector by means of two-phase PIV*, Experiments in Fluids 32, (2002)

[6] Sauter W., Pfeil J., Velji A., Spicher U. et al., *Application of Particle Image Velocimetry for Investigation of Spray Characteristics of an Outward Opening Nozzle for Gasoline Direct Injection*, SAE Technical Paper 2006-01-3377, (2006)

[7] Meinhart C. D., Wereley S. T., Grayl M. H. B., *Volume illumination for two-dimensional particle image velocimetry,* Meas. Sci. Technol. 11: 809-814 (2000)

[8] Olsen M. G., Adrian R. J., O*ut-of-focus effects on particle image visibility and correlation in microscopic particle image velocimetry*, Exp. in Fluids 29(Suppl 1): S166, (2000)

[9] Raffel M., Willert C. E., Wereley S. T., Kompenhans J., *Particle Image Velocimetry*, Springer-Verlag Berlin Heidelberg (2007)

[10] Westerweel J., Scarano F., *Universal outlier detection for PIV data*, Experiments in Fluids 39: 1096–1100, (2005)